

MALAYSIAN JOURNAL OF ANALYTICAL SCIENCES



Journal homepage: https://mjas.analis.com.my/

Research Article

Modification of screen-printed gold electrode based molecularly imprinted polymer (MIP) for 17β-estradiol detection

Julia Hayati Saipol Bahri¹, Tuan Mohamad Fauzan Tuan Omar^{1,2}, Hafiza Mohamed Zuki¹, and Azrilawani Ahmad^{1,2*}

¹Faculty of Science and Marine Environment, Universiti Malaysia Terengganu, 21030 Kuala Nerus, Terengganu, Malaysia ²Ocean Pollution and Ecotoxicology Research Group, Faculty of Science and Marine Environment, Universiti Malaysia Terengganu, 21030 Kuala Nerus, Terengganu, Malaysia

Received: 26 August 2024; Revised: 30 November 2024; Accepted: 12 February 2025; Published: 8 April 2025

Abstract

An efficient approach that integrates a molecularly imprinted conducting polymer, polypyrrole, with a sensitive electrochemical sensing platform for quantifying 17β -estradiol (17β -E2) is presented. The molecular imprinting process employed a one-pot step using the electrochemical polymerisation of pyrrole as a monomer and 17β -E2 as a template molecule, which enabled the control of polymer film thickness, easy adherence of the polymer layers on the sensing substrate, and simplicity of the fabrication on screen-printed gold electrode (SPGE). The molecularly imprinted electrochemical sensor (MIP/SPGE) was characterised physically using scanning electron microscopy and Fourier transform infrared, and it was electrochemically characterised using cyclic voltammetry and linear sweep voltammetry (LSV). The LSV technique was carried out as a detection method because 17β -E2 molecules are electrically insulative and non-electroactive. The MIP/SPGE demonstrates a wide linear detection range, spanning from 0.5 ppm to 10.0 ppm, with a detection limit of 0.00836 ppm and a quantification limit of 0.02785 ppm. The imprinted variant shows a significantly higher affinity for 17β -E2 binding than the non-imprinted sensor. Furthermore, selectivity assessments conducted with testosterone, a similar hormone, confirmed the sensor's high selectivity.

 $\textbf{Keywords}: screen-printed gold electrode, 17\beta-estradiol, polypyrrole, electrochemical polymerisation, molecularly imprinted polymer$

Introduction

Industrial wastewater treatment plants, agricultural run-off, animal feedlots, and residence drainage are significant sources of water pollution worldwide [1], [2]. One of the increasing pollutants is endocrine-disrupting chemicals (EDCs), which can harm the human endocrine system even at low concentrations ranging from ng/L to ug/L [3,4]. EDCs are exogenous compounds that disrupt the normal functioning of the endocrine system by mimicking or inhibiting its operation [5]. The molecules encompass a variety of substances, including endogenous compounds like natural androgens, estrogens and phytoestrogens, as well as an extensive array of synthetic hormones, pharmaceuticals, organochlorine pesticides, and polycyclic aromatic hydrocarbons [2, 6].

Researchers commonly identify the estrogenic

hormone 17β-estradiol (17β-E2) as a prevalent EDC in groundwater and surface water. Studies have discovered that 17β-E2 has carcinogenic properties [7], resulting in the development of abnormal chromosomal structures in human embryonic fibroblast cells [8] and inducing feminisation in male trout [9]. 17β-E2 is classified as a steroidal estrogen because of its chemical structure (C₁₈H₂₄O₂), characterised by four fused rings. The sources of 17β-E2 are varied, encompassing both endogenous production and exogenous sources such administration and environmental release. The ovaries, placenta, and adrenal glands play a crucial role in the endogenous production of hormones in the female body [10]. However, synthetic versions of these hormones are utilised in hormone replacement therapy and contraception [11]. Furthermore, the occurrence of 17β-E2 and its byproducts in the

^{*}Corresponding author: azrilawani.ahmad@umt.edu.my

environment can be ascribed to their discharge through the excretion mechanisms of both humans and animals, thus potentially resulting in the determination of environmental pollution.

The widespread presence of these dangerous compounds in sewage effluents and environmental waters is a major concern for environmental scientists [12]. This is because they have a significant impact on both aquatic life and public health, leading to changes in reproductive function and growth, activation of breast tumours, and other endocrine disorders [11]. Scientists have faced significant challenges in detecting these chemicals due to their frequent occurrence at extremely low concentrations in the sample medium [13]. In addition, the water samples usually contain a diverse range of compounds apart from EDCs, leading to the need for extensive analysis of matrices [14]. Hence, creating a rapid, responsive, accurate and inexpensive technique holds immense significance. Conventional analytical methods, such electrochemiluminescence [15], liquid chromatography-mass [16], spectrometry chemiluminescence immunoassay [17], and the Enzyme-Linked – Immunosorbent Assay [18], have been demonstrated to be highly effective in detecting EDCs due to their exceptional sensitivity and reliability. Nevertheless, all the techniques demonstrated restricted efficacy due to the inherent low ionisation of free estrogens in the complex matrix composition.

Modified electrochemical sensors provide a fast, simple sample preparation, excellent sensitivity, costeffectiveness, and reliable detection technique to address the need for analysing specific EDCs in water samples [19, 20,21]. Applying different nanomaterials and polymers such as gold nanoparticles, multi-walled carbon nanotubes, graphene, and polypyrrole to the electrode surface improves the sensors' selectivity and sensitivity [22]. In recent years, the researcher developed molecularly imprinted polymer (MIP) for electroanalytical purposes [23, 24]. These polymers are considered up-and-coming alternatives to natural receptors. MIPs function through a "lock and key" mechanism, mimicking the molecular process that occurs in biological macromolecules like substrate enzymes or antigen-antibody interactions [25]. Rahman et al. further affirmed that MIPs, as sophisticated polymers, possess the ability to replicate the volume, form, and atomic structure of the template molecule [26]. It provides several advantages, such as the ability to identify a diverse array of targets because of its customised design, enhanced stability in terms of chemical and physical properties, compatibility with organic substances, the potential for reuse, ease of engineering, and affordability [27]. The initial focus of MIP synthesis was on separation and extraction techniques. However, with constant advances and research, these novel substances have found applications in various domains. These include the fabrication of sensors, immunoassays, controlled drug release, direct synthesis, catalysis, cell and tissue imaging, and even in the field of medicine [28]. The advancement of molecularly imprinted electrochemical sensors through the integration of MIP and electrochemistry has resulted in improved sensor performance, enabling the use of redox probes as the basis for both in-situ and ex-situ detection via a variety of electroanalytical techniques, including conductometry, voltammetry, amperometry, and potentiometry [29].

The molecular imprinting method is succinct; it entails the copolymerisation of a functional monomer or a sequence of monomer units with an initiator and a cross-linker in the presence of template molecules [30] either by covalent, semi-covalent, or noncovalent approach [31] using various polymerisation techniques such as electropolymerisation [32], sol-gel [33], and suspension [34]. The functional monomer must possess distinct functional groups capable of forming bonds with the template molecules [35]. The procedure involves removing the template from the polymer through either chemical breakdown or solvent extraction to endow the MIPs with stable binding capabilities [36]. Afterward, the polymer matrix generates a region containing chemical functional groups and dimensions similar to the template. This region facilitates the MIPs' recognition of specific molecular analytes.

In this research study, we constructed a novel MIP-based electrochemical sensor with high selectivity and sensitivity. A MIP film was fabricated onto the screen-printed gold electrode (SPGE) for efficient selective detection of $17\beta\mbox{-}E2$ in real samples by covalent approach via electropolymerisation technique.

Materials and Methods Reagents and apparatus

All chemicals were of analytical reagent grade and used without further purification. Deionised water was used throughout the research work. 17β -E2 was purchased from Thermo Fischer Scientific (United States). A solution of 17β -E2 (1.0×10 –2 mol/L) was obtained in ethanol. Pyrrole and lithium perchlorate were bought from Sigma Aldrich (United States). Acetic acid (Glacial), potassium-ferricyanide, ethanol, and methanol were bought from R & M Chemical (United Kingdom). Potassium chloride was purchased from Merck (Germany). Scanning electron microscopy (SEM; TESCAN VEGA) was used to research the morphology of modified materials. Autolab PGSTAT302N (Metrohm) was used to carry out all electrochemical measurements. C220AT

SPGEs were purchased from Metrohm DropSens. They consisted of a three-electrode system with a gold working electrode (0.19 cm²), a saturated Ag/AgCl reference electrode, and a gold plate counter electrode (0.54 cm²).

Fabrication of MIP/SPGE

The electrode was first immersed in ethanol/deionised water (50:50) v/v solution for a minute to remove the impurities on the surface of the electrode, as prescribed by Motia et al. [37]. The SPGE was washed with deionised water several times and dried in an atmosphere before the fabrication process. The MIP film was electropolymerised by immersing the cleaned electrode into 0.1 M lithium perchlorate solution containing 0.015 M of the monomer (pyrrole) and 0.01 mM of the template (17β-E2/ethanol) via cyclic voltammetry (CV) for (three cycles) between – 0.4 V and 0.8 V at a scan rate of 10 mV/s. The prepolymerisation solution was purged with nitrogen gas for 5 min to eliminate the presence of oxygen in the solution and ensure the successfulness of the MIP fabrication on the working electrode before the electropolymerisation process. The NIP layer was synthesised similarly on the SPGE without adding estradiol as the template molecule. The template molecular molecule (17β-E2) was then removed by immersing the SPGE working electrode with methanol/acetic acid (9:1) v/v solution, as recommended by Muhammad et al [38].

Electrochemical characterisation method

experiments electrochemical for characterisation using modified electrodes were performed in 0.1 M KCl solution containing 0.5×10^{-2} mol L^{-1} [Fe (CN)₆]^{3-/4-} as a redox probe in the potential range of -0.2 V to +0.4 V with a scan rate of 100 mV/s based on a previous study by Duan et al. [39]. The reaction was conducted under normal atmospheric conditions without specific requirements such as air or mixture exclusion. The linear sweep voltammetry (LSV) experiments for selectivity study and 17β-E2 detections utilising MIP/SPGE and NIP/SPGE were conducted in the potential range of 0.5 V to 1.5 V at a scan rate of 100 mV/s as research demonstrated in the work of Supchocksoonthorn et al. [40] with some modifications.

Physical characterisation method

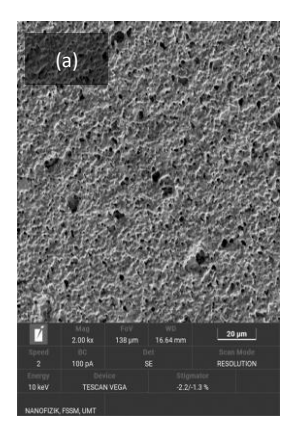
SEM analysis was performed using a TESCAN VEGA scanning electron microscope. The imaging

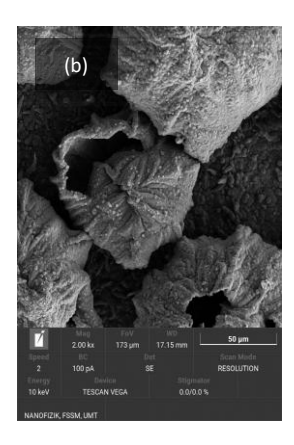
was conducted under high vacuum conditions with an accelerating voltage of 10 keV to ensure highresolution images of the polymer film surface morphology. The working distance was maintained at 5 mm, and secondary electron mode was used to capture detailed topographical information. Images were taken at a magnification of 2000x to observe the overall surface structure and finer details of the polymer film fabricated on the working electrode of Fourier transformed infrared (FTIR) spectroscopy analysis was performed using a Fourier transform infrared spectroscopy - attenuated total reflectance (FTIR-ATR) (IRTracer-100 Shimadzu model), spanning a wavenumber range of 4000-400 cm⁻¹, with each sample subjected to 30 scans to ensure reproducibility. The spectra were analysed to identify the characteristic absorption bands of specific functional groups, elucidating the interactions between the template molecules and monomers in the MIP polymer compared to the NIP polymer fabricated on SPGE.

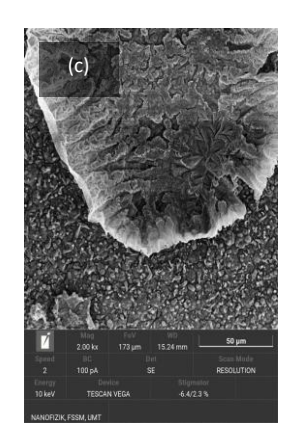
Results and Discussion

Surface morphology of bare and modified screenprinted electrode

The surface morphology of bare SPGE, MIP/SPGE before template removal, MIP/SPGE after template removal, and NIP/SPGE were investigated through SEM. Figure 1(a) depicts SEM images of the working electrode surface on the bare SPGE employed rough appearance with small pores [41]. Figure 1(b) and Figure 1(c) represent the SEM image of the MIPmodified electrode before and after the template removal process. The deposition of 17β-E2 (Figure 1(b)) on the surface of the electrode is confirmed by the presence of a nanoparticle with size 90 µm attached to the surface before template removal using methanol/acetic acid (9:1) v/v solution. The irregular structure. Figure 1(c) on the surface MIP/SPGE indicates the removal of the template molecule, specifically the 17β-E2. These morphological characteristics are critical for the electrode's performance in electrochemical applications, as they influence the surface area and the accessibility of the active sites for analyte interaction [42]. Figure 1(d) of NIP/SPGE shows that the spheres possess coarse surfaces with a diameter distribution of 0.5 to 2 μm, indicating the even deposition layer of polypyrrole nanoparticles on the surface of the working electrode. The surface morphology observed is consistent with the expected structure of electropolymerised pyrrole derivatives, as conducted by Shafaat et al. [43].







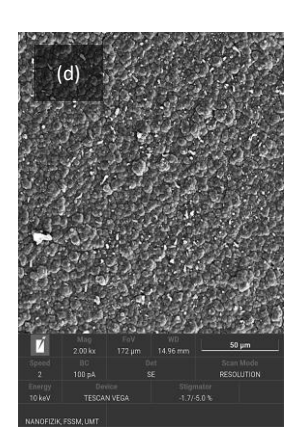


Figure 1. (a) SEM morphology of bare SPGE, (b) MIP/ SPGE prior to template removal, (c) MIP/ SPGE after template removal, and (d) NIP/ SPGE

FTIR analysis of electropolymerised polymers on SPGE

Figure 2 compares the FTIR spectra between the MIP before template removal, MIP after template removal and the NIP polymer. The MIP before the template removal spectra exhibits a distinctive and wide peak centred at 3340.71 cm⁻¹, attributed to the overlapping of O-H stretching vibrations from the 17β-E2 molecules. An irregular peak at 1095.57 cm⁻¹ is also observed for the MIP before template removal, which can be attributed to C-O stretching vibrations associated with ether or alcohol groups; this peak diminishes after the template removal, indicating the loss of interactions involving oxygen-containing groups. The NIP exhibits medium bands at 3332.99 cm⁻¹, which can be ascribed to the N-H stretching vibration associated with the presence of pyrrole [44]. The FTIR spectra of both MIP before template removal and NIP show a peak at 663.51 cm⁻¹, attributed to hydrogen bonding resulting from the halogen molecule Cl found in the lithium perchlorate used as a supporting electrolyte during the electropolymerisation procedure [45]. comparison with the MIP after template removal, the broad peak of the hydroxyl group at 3340.71 cm⁻¹ diminishes, and the spectra reveal a peak at 3332.99 cm⁻¹, indicating a shift towards the N-H group. A small peak at 1635.64 cm⁻¹, similar to that observed in both the MIP before template removal and the NIP, is present. This peak can be attributed to the C=C stretching vibrations, which are characteristic of aromatic or alkene groups, suggesting that it is a structural feature of the polymer backbone [45]. The peak at 663.51 cm⁻¹ remains evident, suggesting persistent hydrogen bonding. Table 1 compares the absorption peaks of electropolymerised polymers fabricated on SPGE.

Electrochemical characterisation of modified electrodes

The electrochemical response of bare and modified electrodes was characterised using CV in a 0.5×10^{-2} mol L^{-1} [Fe (CN)₆]^{3-/4-} solution containing 1 × 10-1 mol/L potassium chloride, as shown in **Figure 3**. The $[Fe (CN)_6]^{3-/4-}$ solution was utilised as an intermediary to evaluate the voltammetric responses of electrodes by connecting various modified electrodes with substrate solutions. The peak for bare electrode was represented by the smallest voltammogram and lowest peak current intensity indicate limited electrochemical activity (Figure 3(a)). Conversely, the MIP/SPGE before template removal (Figure 3(b)) showed a more pronounced response, with electrochemical a larger voltammogram than the bare electrode. This enhancement is due to the presence of the electropolymerised polypyrrole layer and the embedded 17\u03b3-E2 molecules, which improve the overall conductivity and surface area of the electrode [46]. However, the peak current and voltammogram size were smaller than the modified electrode after template removal, as the template molecules partially block the conductive pathways. After the template removal procedure using methanol/acetic acid (9:1) v/v, the MIP/SPGE (Figure 3(c)) displayed the most significant electrochemical response, characterised by the largest and broadest voltammogram with the highest peak current intensity. The distinct peak shape elucidates a well-defined redox process, suggesting that the 17β-E2 removal created specific recognition sites and enhanced the electrode's conductivity [47]. The recognition sites available facilitate the efficient transfer of electrons, leading to a more pronounced electrochemical signal. NIP/SPGE (Figure 3(d)) showed a slightly different electrochemical behaviour, with a more tapered peak shape than bare and other modified electrodes. The absence of 17\beta-E2 as the

template molecule during the polymerisation process resulted in a uniform polypyrrole layer without specific recognition sites [48, 49]. This results in a more homogeneous but less conductive surface than MIP/SPGE. Ergo, the electrochemical response is less pronounced than that of the MIP/SPGE but better than the bare SPGE.

The CVs of MIP/SPGE (**Figure 4(a)**) and NIP/SPGE (**Figure 4(c)**) were obtained at various scanning rates ranging from 10 to 100 mV/s. The measurements were conducted in 0.5×10^{-2} mol/L [Fe (CN)₆]^{3-/4}– containing 1×10^{-1} mol/L KCl solution to study the electrochemical behaviour of the sensor. The redox peak current of both modified electrodes was proportional to the scanning rate, as seen in **Figure 4(b)** and **Figure 4(d)**. Furthermore, the linear equation of MIP/SPGE can be expressed as I_{pa} (y) = 3E-06x +

1E-05 (R^2 = 0.9972) and I_{pc} (y) = -3E-06x - 3E-05 (R^2 = 0.9885). The NIP/SPGE recorded I_{pa} (y) = 2E-06 x + 5E-05 (R² = 0.9708) and I_{pc} (y)= -2E-06x - 6E -05 $(R^2 = 0.9829)$. The results indicated a surfaceconfined electrochemical phenomenon of the process [34]. The consistent electrochemical response of both modified electrodes across various scan rates ensures reliable detection and quantification of 17β-E2 in complex samples, particularly in environmental water, highlighting its potential as a promising portable sensor for in-situ detection of 17 β -E2 [50]. The higher linearity observed for MIP/SPGE in both anodic peak current (Ipa) and cathodic peak current (Ipc) as a function of the scan rate indicates that the electron transfer between the electrode and the redox species in the solution is more rapid and efficient compared to NIP/SPGE [51].

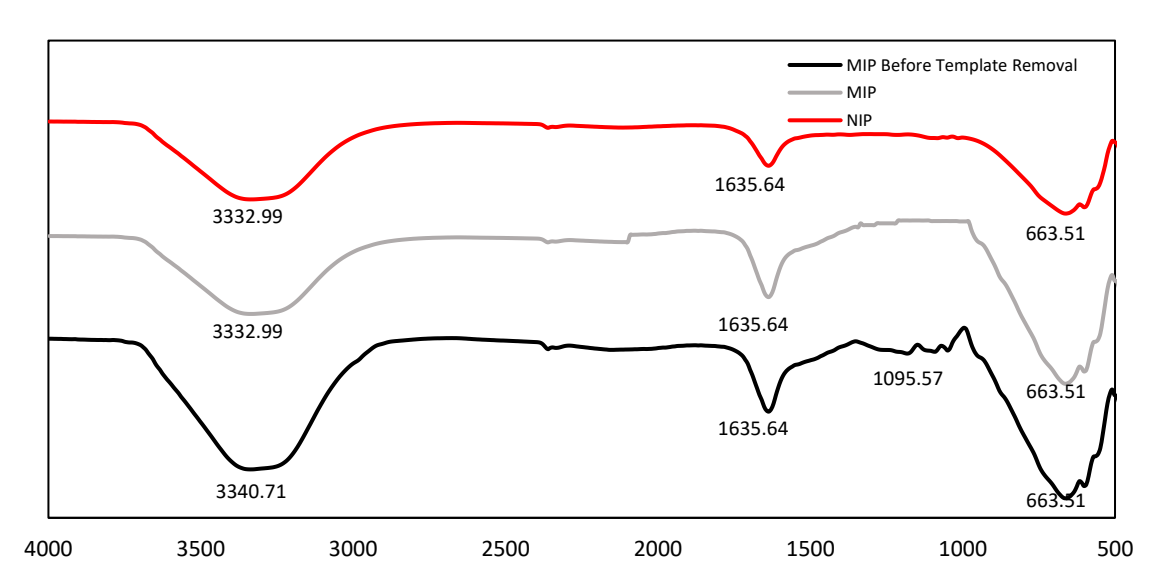


Figure 2. FTIR spectra of MIP before template removal and of the MIP and NIP

Table 1. Functional groups associated with absorption peaks in electropolymerised polymer on SPGE

| Absorption Peak (cm ⁻¹) | Functional Group | MIP Before Template Removal | MIP | NIP |
|-------------------------------------|------------------|--------------------------------|---------|---------|
| | 0.11 | | A.1 | A.1 |
| 3340.71 | О-Н | Present | Absent | Absent |
| 3332.99 | N-H | Present | Present | Present |
| 1635.64 | C=C | Present | Present | Present |
| 1095.57 | C-O | Present | Absent | Absent |
| 663.51 | Hydrogen bonding | Present | Present | Present |
| | (Cl as acceptor) | | | |

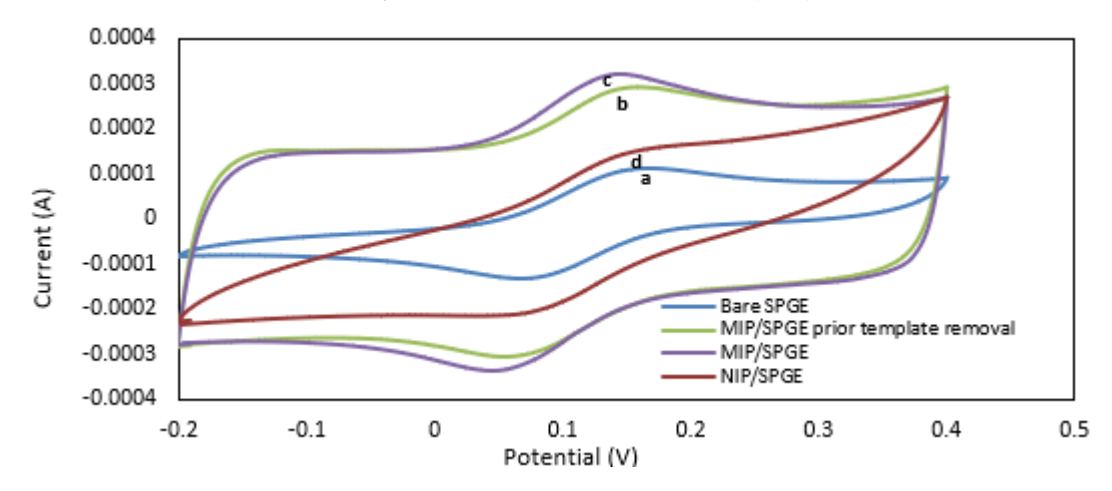
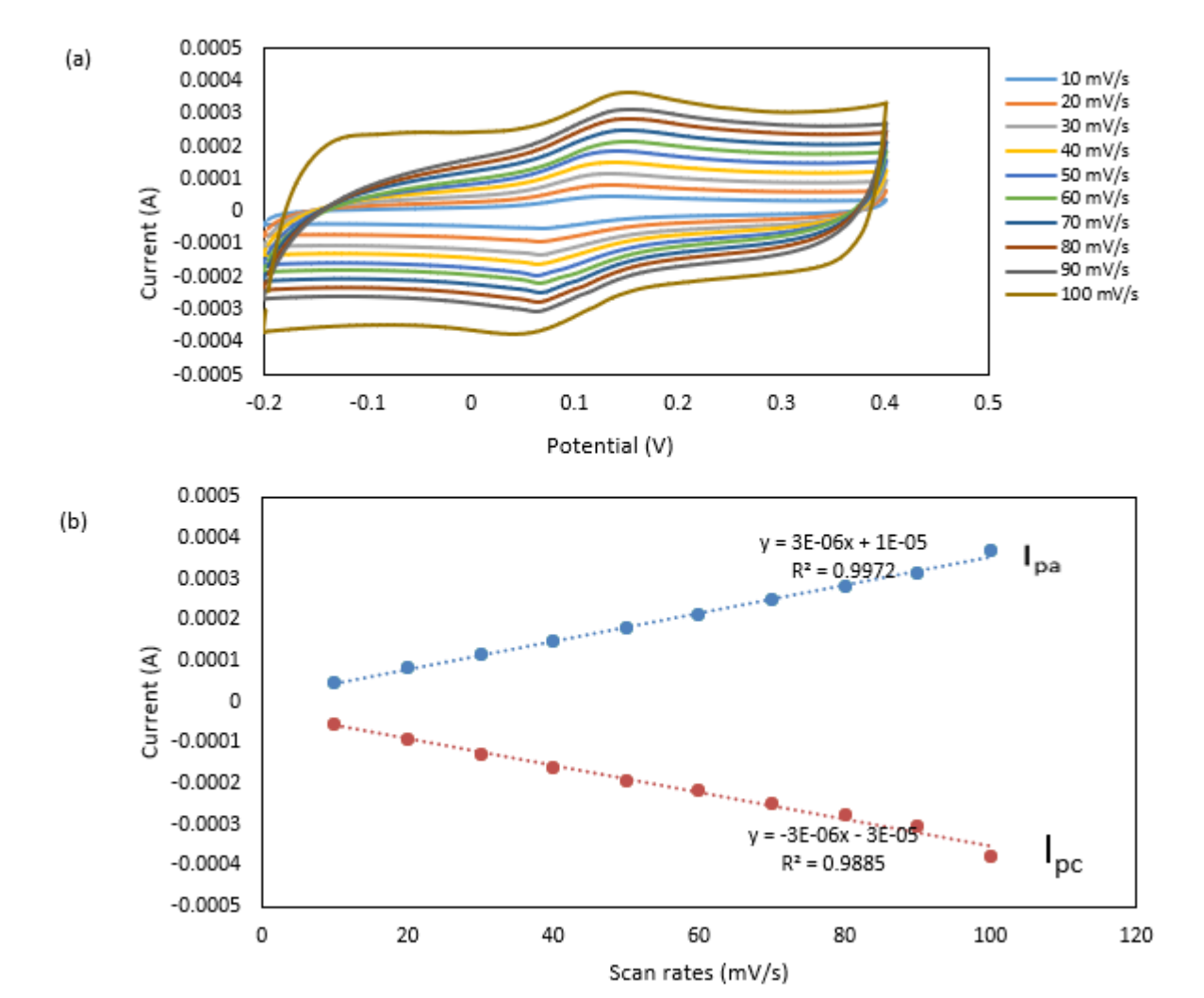


Figure 3. CV of the various electrodes: (a) bare SPGE, (b) MIP/SPGE before template removal, (c) MIP/SPGE after template removal, and (d) NIP/SPGE at 100 mV/s scan rate in a 0.5×10^{-2} mol L⁻¹ [Fe (CN)₆]^{3-/4-} solution that contains 1×10^{-1} mol/L KCl



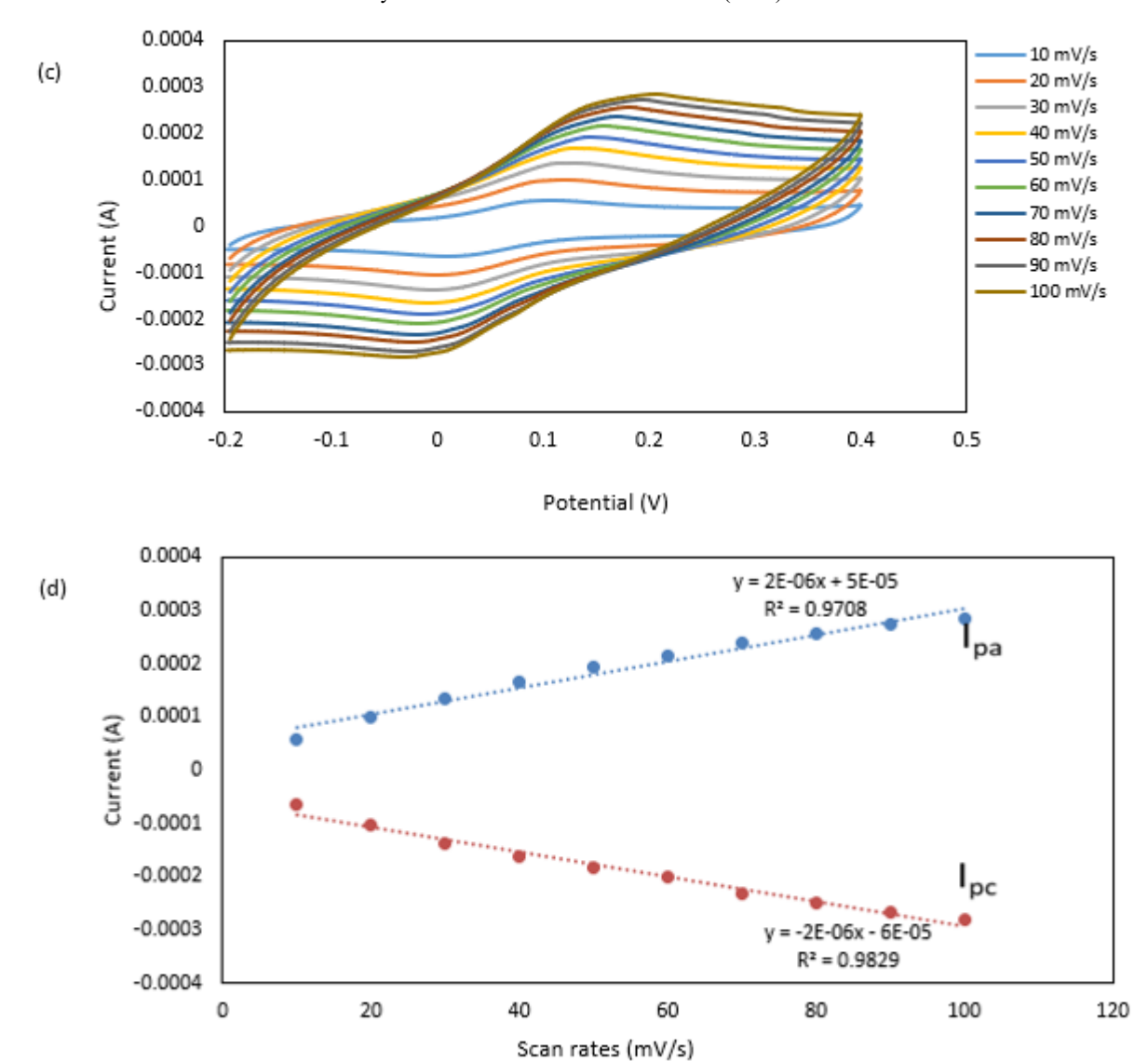


Figure 4. (a) CV results for MIP/SPGE sensor at various scanning rates (from outer to inner): 10, 20, 30, 40, 50, 60, 70, 80, 90 and 100 mV/s. (b) Resultant calibration plots of MIP/SPGE among different scanning rates vs. cathodic and anodic peak currents. (c) CV results for NIP/SPGE sensor at various scanning rates (outer to inner): 10, 20, 30, 40, 50, 60, 70, 80, 90 and 100 mV/s. (d) Resultant calibration plots of NIP/SPGE among different scanning rates vs. cathodic and anodic peak currents. All measurements were obtained using a 0.5×10^{-2} mol/L [Fe (CN)₆]^{3-/4}— solution that contains 1×10^{-1} mol/L KCl

Optimisation of analytical conditions

Several parameters were optimised, such as the choice of monomer concentration, scan cycles, scan rates and template removal incubation time, to analyse their effects on the fabrication process.

Monomer concentration

The tests were performed in triplicate, and the results are expressed in **Figure 5(a)**. It was observed that the increase in the monomer pyrrole concentration increases the sensor response with a stabilisation of around 0.015 M. The amount of pyrrole functional

monomers was varied while keeping the template molecule, 17β -E2, constant. The current resulting from the rebinding experiment was recorded and revealed that the sensor's performance greatly varies. The peak current gradually declines as the concentration of the pyrrole monomer increases. The formulation gave a high peak current by employing 0.015 M of pyrrole during electropolymerisation. The conjugated π electrons in the pyrrole ring can easily participate in electron transfer reactions, enhancing the flow of electrons at the interface between the solution and electrode surface [32]. The more pyrrole

rebinds to the film, the higher the current signals confirming that there are specific binding sites formed on the polymer films [52] All these changes in the current densities confirm the formation of the imprinted electropolymerised thin film on the surface of the SPGE working electrode, which can recognise and quantify the template.

Scan cycles

The number of scan cycles significantly influences the thickness and density of the polymer film deposited on the electrode surface. With an increase in scan cycles, the polymer film tends to become thicker as more MIP molecules undergo polymerisation and deposition [53]. However, an excessively thin MIP film restricts the availability of imprinted sites, while an overly thick film can trap the template molecules too deeply, obstructing their accessibility [52]. As illustrated in **Figure 5(b)**, the optimal current response was achieved with three scan cycles. Increasing the number of scan cycles to five and seven resulted in a decline in peak current, which was attributed to the degradation of the SPGE.

Scan rates

The scan rate in CV significantly impacts the electropolymerisation process of MIP molecules during the formation of conductive polymer films. The scan rate affects the morphology of the polymer film. Lower scan rates generally provide better control over film morphology, resulting in more compact and well-organised structures [54]. Higher scan rates lead to less controlled growth and a more disordered film. Figure 5(c) shows that the peak current produced is inversely proportional to the scan rates applied during the electropolymerisation process. These occurred due to the formation of non-uniform and less binding sites on the surface of the polymer with higher scan rates [32]. The scan rate of 10 mV/s was chosen as the optimum rate to electropolymerise the MIP molecules on the SPGE because the 5 mV/s scan rate tends to degrade and corrode the SPGE.

Template removal time

The optimum period for template $(17\beta\text{-E2})$ extraction was investigated at varied times from 1 minute to 4 hours. The mixture of methanol/acetic acid 9:1 (v/v) solution was used as an extracting solvent. The acidic and corrosive properties of the acetic acid solution weaken the weak non-covalent interaction of hydrogen bonding of the template molecule $17\beta\text{-E2}$ and the polypyrrole film [55]. The peak current obtained is presented in **Figure 5(d)**. The 1-minute washing process for template removal corresponds to the highest number of imprinted sites produced. A prolonged period exceeding 1 minute caused the continuous decline in peak current produced due to the excessive degradation of the working electrode.

17β-estradiol detection using the modified sensor The linearity of the MIP/SPGE (Figure 6(a); Figure 6(b)) and NIP/SPGE (Figure 6(c); Figure 6(d)) sensor was evaluated using LSV across various concentrations of 17β-E2, ranging from 0.5 ppm to 10.0 ppm. The peak current increased proportionally with the increase of 17β-E2 concentration, as shown in the analytical plot of Figure 6(b). The calibration curve for the MIP/SPGE sensor was represented by the equation y = 0.0002x with a high correlation coefficient $R^2 = 0.98$. The sensor demonstrated a detection limit (LOD) of 0.00836 ppm and a limit of quantification (LOQ) of 0.02785 ppm, determined using established methodologies [56]. The NIP/SPGE calibration curve (Figure 6(d)) was y = 3E-05x +0.0003 with an R2 value of 0.9772. The lower sensitivity and different slope of the NIP/SPGE sensor, as indicated by its calibration curve, highlight the enhanced performance and specificity of the MIP/SPGE sensor towards 17β-E2. This distinction underscores the significance of the molecular imprinting process in developing selective and sensitive sensors for specific target analytes [26]. **Table 2** compares the experimental findings for both MIP/SPGE and NIP/SPGE sensors, elucidating the superior analytical performance of the MIP/SPGE sensitivity, detection limit regarding quantification limit.

Table 2. Electrochemical properties of modified sensors for 17β -E2 detection

| Sensor | LOD (ppm) | LOQ (ppm) | Linear Range (ppm) | R^2 | σ blank (A) |
|----------|-----------|-----------|--------------------|--------|-------------------------|
| MIP/SPGE | 0.00836 | 0.02785 | 0.5-10.0 | 0.98 | 5.57 x 10 ⁻⁷ |
| NIP/SPGE | 0.153 | 0.510 | 0.5-10.0 | 0.9772 | 2.55 x 10 ⁻⁶ |

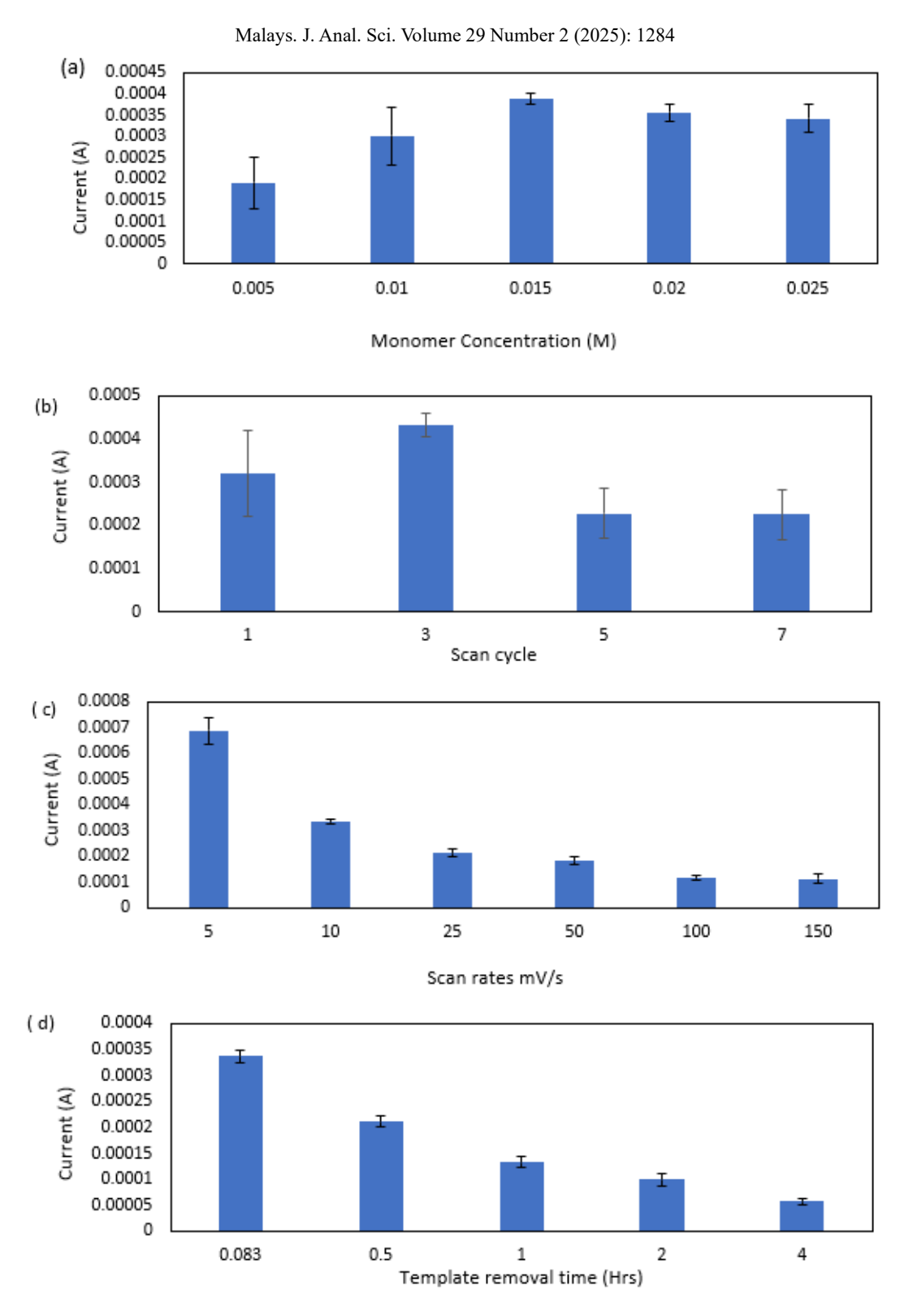


Figure 5. The effects of (a) monomer concentration, (b) scan cycle, (c) scan rates, and (d) template removal period on the current response of MIP/SPGE

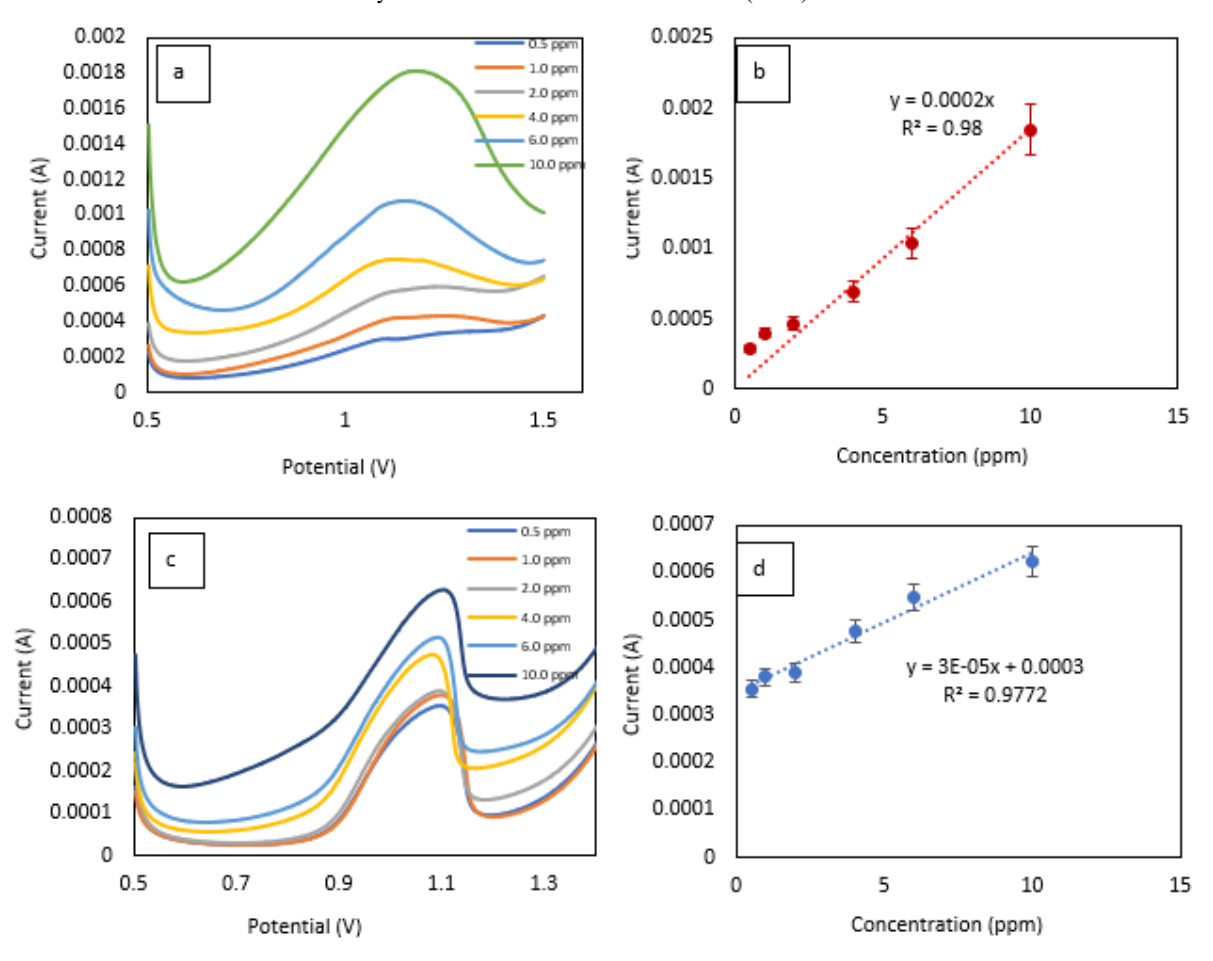


Figure 6. (a) Linear sweep voltammetry diagrams of MIP/SPGE for increasing 17β-E2 concentrations; (b) linear calibration graph of 17β-E2; (c) linear sweep voltammetry diagrams of NIP/SPGE for increasing 17β-E2 concentrations; (d) linear calibration graph of 17β-E2

Reproducibility, stability and selectivity of the MIP/SPGE

Seven modified electrodes were fabricated using the same electropolymerisation procedure using the optimised parameters. To assess their consistency and reproducibility, CV measurements were performed in a solution of $0.5 \times 10^{-2} \text{ mol/L } [\text{Fe}(\text{CN})_6]^{3./4}$ - containing $1 \times 10^{-1} \text{ mol/L M KCl}$. The current responses of the electrodes remained nearly constant across the tests, as demonstrated in **Figure 7(a)**, with a relative standard deviation (RSD) of 5.83%. This low RSD value indicates minimal sensor-to-sensor variation, suggesting that the proposed fabrication method provides high reproducibility and consistent quality for the modified electrodes.

The storage stability of three modified sensors was evaluated over 20 days at 8°C, with measurements taken every two days (**Figure 7(b)**). The average activity of the sensors was maintained at 94±10% of

the initial value for the first 14 days. The stability of the modified dropped drastically to 51% from the first day of stability testing after day 14 and continued to decline until 20 days of storage. The results demonstrate that MIP electrodes may be reused at least seven times without substantial degradation in relative current response.

The selectivity of the modified electrode was tested by comparing its current responses to 0.01 M 17 β -E2 and 0.01 M testosterone using LSV. The electrode exhibited a significantly higher current response for 17 β -E2 (0.00128 A) than testosterone (0.00038 A), as depicted in **Figure 7(c)**. This indicates the modified electrode's higher affinity and selectivity towards 17 β -E2, likely due to the specific molecular imprinting process that creates binding sites tailored for 17 β -E2[57]. The enhanced selectivity is crucial for accurately and reliably detecting 17 β -E2 in the presence of other potentially interfering substances.

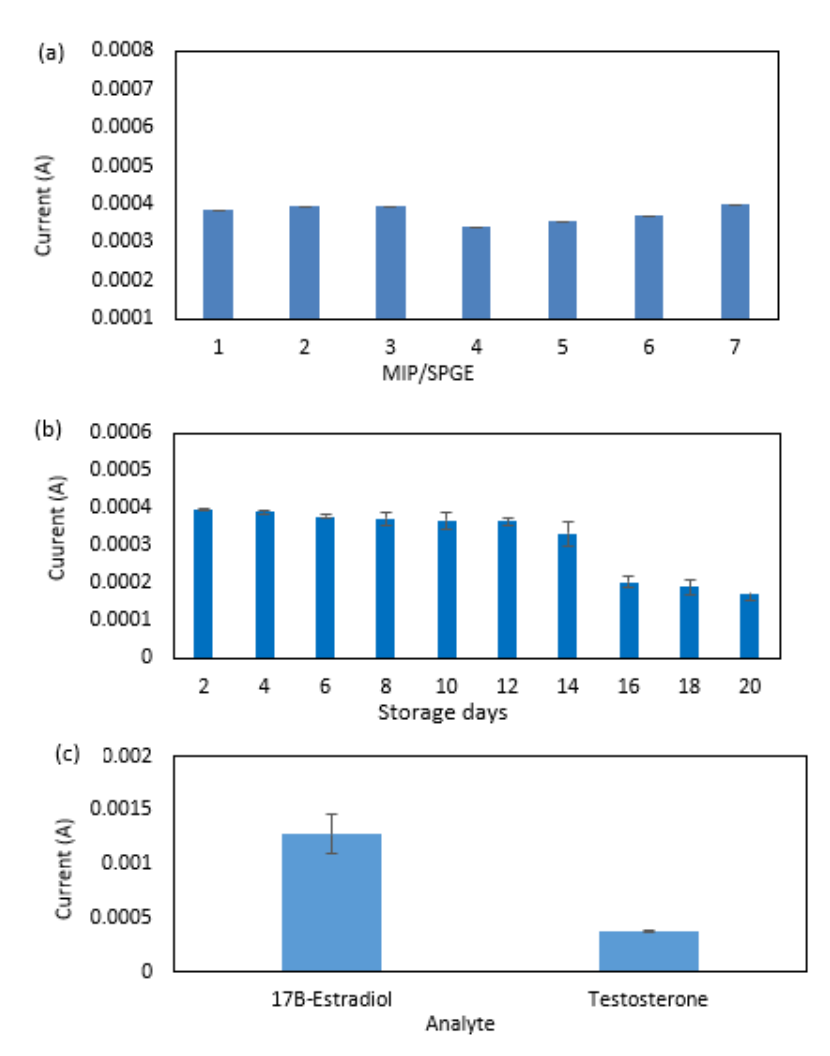


Figure 7. (a) Reproducibility test, (b) stability test, and (c) selectivity test of MIP/SPGE towards 17β-E2

Conclusion

A sensitive molecularly imprinted electrochemical sensor was developed to detect estradiol using electropolymerisation 17β -Estradiol/polypyrrole on the SPGE. This straightforward preparation resulted in a MIP sensor with a broad linear range, high sensitivity, selectivity and reproducibility. Moreover, the analysis of complex matrices demonstrated the MIP sensor's applicability for detecting 17β -Estradiol in river water samples. The developed MIP-based sensor is easy to fabricate and operate and exhibits high sensitivity and selectivity.

Acknowledgment

The authors would like to acknowledge the financial support the Universiti Malaysia Terengganu provided through the Talent and Publication Enhancement Research Grant (UMT/TAPE-RG/2021/55322), which facilitated the successful completion of this research.

References

- Kaya, S. I., Cetinkaya, A., Bakirhan, N. K., and Ozkan, S. A. (2020). Trends in sensitive electrochemical sensors for endocrine disruptive compounds. *Trends in Environmental Analytical Chemistry*, 28: e00106.
- Omar, T. F. T., Ahmad, A., Aris, A. Z., and Yusoff, F. M. (2016). Endocrine disrupting compounds (EDCs) in environmental matrices: Review of analytical strategies for pharmaceuticals, estrogenic hormones, and alkylphenol compounds. *TrAC Trends in Analytical Chemistry*, 85: 241-259.
- 3. Ismail, N. A. H., Aris, A. Z., Wee, S. Y., Nasir, H. M., Razak, M. R., Kamarulzaman, N. H., and Omar, T. F. T. (2021). Occurrence and distribution of endocrine-disrupting chemicals in mariculture fish and the human health implications. *Food Chemistry*, 345: 128806.
- 4. Chen, Y., Yang, J., Yao, B., Zhi, D., and Zhou, Y. (2022). Endocrine disrupting chemicals in the

- environment: Environmental sources, biological effects, remediation techniques, and perspective. *Environmental Pollution*. 310: 119918.
- 5. Van Cauwenbergh, O., Di Serafino, A., Tytgat, J., and Soubry, A. (2020). Transgenerational epigenetic effects from male exposure to endocrine-disrupting compounds: A systematic review on research in mammals. *Clinical Epigenetics*, 12(1): 1-23.
- Su, C., Cui, Y., Liu, D., Zhang, H., and Baninla, Y. (2020). Endocrine disrupting compounds, pharmaceuticals and personal care products in the aquatic environment of China: Which chemicals are the prioritized ones? Science of the Total Environment, 720: 137652.
- Calaf, G. M., Ponce-Cusi, R., Aguayo, F., Muñoz, J. P., and Bleak, T. C. (2020). Endocrine disruptors from the environment affecting breast cancer (Review). *Oncology Letters*, 20(1): 19-32.
- 8. Lucaccioni, L., Trevisani, V., Marrozzini, L., Bertoncelli, N. B. P., Lugli, L., Berardi, A., and Iughetti, L. (2020). Endocrine-disrupting chemicals and their effects during female puberty: A review of current evidence. *International Journal of Molecular Sciences*, 21(6): 2078.
- 9. Adeel, M., Song, X., Wang, Y., Francis, D., and Yang, Y. (2017). Environmental impact of estrogens on human, animal and plant life: A critical review. *Environment International*, 99: 107-119.
- Richards, J. S., and Pangas, S. A. (2010). The ovary: Basic biology and clinical implications. *Journal of Clinical Investigation*, 120(4): 963-972.
- 11. Nazari, E., and Suja, F. (2016). Effects of 17β-estradiol (E2) on aqueous organisms and its treatment problem: A review. *Reviews on Environmental Health*, 31(4): 465-491.
- Sabri, M. M., Omar, T. F. T., Ahmad, A., and Suratman, S. (2022). An optimized analytical method to study the occurrence and distribution of bisphenol A (Bpa) and 17ß-Estradiol (E2) in the surface water of Ibai River, Terengganu, Malaysia. *Journal of Sustainability Science and Management*, 17(7): 195-203.
- 13. Dong, Z., Xiao, C., Zeng, W., and Zhao, J. (2021). Impact of 17β-Estradiol on natural water's heterotrophic nitrifying bacteria. *International Journal of Environmental Science and Development*, 12(1): 17-22.
- 14. Özgür, E. (2021). Molecularly imprinted electrochemical sensors and their applications. *Molecular Imprinting for Nanosensors and Other Sensing Applications*, 2021: 203-221.
- 15. Zhang, J. J., Cao, J. T., Shi, G. F., Huang, K. J., Liu, Y. M., and Chen, Y. H. (2014). Label-free and sensitive electrochemiluminescence

- aptasensor for the determination of 17β -estradiol based on a competitive assay with cDNA amplification. *Analytical Methods*, 6(17): 6796-6801.
- Wang, L., Yang, P., Li, Y., and Zhu, C. (2006). A flow-injection chemiluminescence method for the determination of some estrogens by enhancement of luminol-hydrogen peroxide-tetrasulfonated manganese phthalocyanine reaction. *Talanta*, 70: 219-224.
- Li, Y., Yang, L., Zhen, H., Chen, X., Sheng, M., Li, K., Xue, W., Zhao, H., Meng, S., and Cao, G. (2021). Determination of estrogens and estrogen mimics by solid-phase extraction with liquid chromatography-tandem mass spectrometry. *Journal of Chromatography B: Analytical Technologies in the Biomedical and Life Sciences*, 1168: 122559.
- 18. Silva, C. P., Lima, D. L. D., Schneider, R. J., Otero, M., and Esteves, V. I. (2013). Development of ELISA methodologies for the direct determination of 17β-estradiol and 17αethinylestradiol in complex aqueous matrices. *Journal of Environmental Management*, 124: 121-127.
- Alberti, G., Zanoni, C., Spina, S., Magnaghi, L. R., and Biesuz, R. (2022). MIP-based screenprinted potentiometric cell for atrazine sensing. *Chemosensors*, 10(8): 1-15.
- Sarpong, K. A., Zhang, K., Luan, Y., Cao, Y., and Xu, W. (2019). Development and application of a novel electrochemical sensor based on AuNPs and Difunctional monomer-MIPs for the selective determination of Tetrabromobisphenol-S in water samples. *Microchemical Journal*, 104526.
- Rebocho, S., Cordas, C. M., Viveiros, R., and Casimiro, T. (2018). Development of a ferrocenyl-based MIP in supercritical carbon dioxide: Towards an electrochemical sensor for bisphenol A. *Journal of Supercritical Fluids*, 135: 98-104.
- 22. Ni, X., Tang, X., Wang, D., Zhang, J., Zhao, L., Gao, J., He, H., and Dramou, P. (2023). Research progress of sensors based on molecularly imprinted polymers in analytical and biomedical analysis. *Journal of Pharmaceutical and Biomedical Analysis*, 235: 115659.
- 23. Musa, A. M., Kiely, J., Luxton, R., and Honeychurch, K. C. (2021). Recent progress in screen-printed electrochemical sensors and biosensors for the detection of estrogens. *TrAC Trends in Analytical Chemistry*, 139: 116254.
- 24. Mokni, M., Mazouz, Z., Attia, G., Fourati, N., Zerrouki, C., Othmane, A., Omezzine, A., and Bouslama, A. (2018). Prime importance of the supporting electrolyte in the realization of molecularly imprinted polymers. *International*

- Conference on Multidisciplinary Sciences, 1: 5888
- 25. Belbruno, J. J. (2019). Molecularly imprinted polymers. *Chemical Reviews*, 119(1): 94-119.
- 26. Rahman, S., Bozal-Palabiyik, B., Unal, D. N., Erkmen, C., Siddiq, M., Shah, A., and Uslu, B. (2022). Molecularly imprinted polymers (MIPs) combined with nanomaterials as electrochemical sensing applications for environmental pollutants. *Trends in Environmental Analytical Chemistry*, 36(8): e00176.
- 27. Yarman, A., and Scheller, F. W. (2020). How reliable is the electrochemical readout of MIP sensors? *Sensors* (Switzerland), 20(9): 2677.
- 28. Suryanarayanan, V., Wu, C. T., and Ho, K. C. (2010). Molecularly imprinted electrochemical sensors. *Electroanalysis*, 22(16): 1795-1811.
- 29. Cui, B., Liu, P., Liu, X., Liu, S., and Zhang, Z. (2020). Molecularly imprinted polymers for electrochemical detection and analysis: progress and perspectives. *Journal of Materials Research and Technology*, 9(6): 12568-12584.
- 30. Włoch, M., and Datta, J. (2019). Synthesis and polymerisation techniques of molecularly imprinted polymers. *Comprehensive Analytical Chemistry*, 86: 17-40.
- 31. Abdollah, N. A., Ahmad, A., and Omar, T. F. T. (2020). Synthesis and characterization of molecular imprinted polymer for the determination of carbonate ion. *Biointerface Research in Applied Chemistry*, 11(3): 10620-10627.
- 32. Biyana, M., and Nyokong, T. (2022). Synergistic recognition and electrochemical sensing of 17 β-Estradiol using ordered molecularly imprinted polymer-graphene oxide-silver nanoparticles composite films. *Journal of Electroanalytical Chemistry*, 922.
- 33. Khosropour, H., Saboohi, M., Keramat, M., Rezaei, B., and Ensafi, A. A. (2023). Electrochemical molecularly imprinted polymer sensor for ultrasensitive indoxacarb detection by tin disulfide quantum dots/carbon nitride/multiwalled carbon nanotubes as a nanocomposite. Sensors and Actuators B: Chemical, 385(3): 133652.
- 34. Korol, D., Kisiel, A., Cieplak, M., Michalska, A., Sharma, P. S., and Maksymiuk, K. (2023). Synthesis of conducting molecularly imprinted polymer nanoparticles for estriol chemosensing. *Sensors and Actuators B: Chemical*, 382(2): 133476.
- 35. Murdaya, N., Triadenda, A. L., Rahayu, D., and Hasanah, A. N. (2022). A review: Using multiple templates for molecular imprinted polymer: Is it good? polymers, 14(20): 1-22.
- 36. Ellwanger, A., Berggren, C., Bayoudh, S., Crecenzi, C., Karlsson, L., Owens, P. K., Ensing,

- K., Cormack, P., Sherrington, D., and Sellergren, B. (2001). Evaluation of methods aimed at complete removal of template from molecularly imprinted polymers. *Analyst*, 126(6): 784-792.
- 37. Motia, S., Bouchikhi, B., Llobet, E., and El Bari, N. (2020). Synthesis and characterization of a highly sensitive and selective electrochemical sensor based on molecularly imprinted polymer with gold nanoparticles modified screen-printed electrode for glycerol determination in wastewater. *Talanta*, 216(3): 120953.
- 38. Nabilah Muhamad, F., Mohamed Zuki, H., Ariffin, M., and Ahmad, A. (2023). Molecularly imprinted polymers for domoic acid detection in selected shellfish tissue. *Malaysian Journal of Analytical Sciences*, 27(2): 353-367.
- 39. Duan, D., Si, X., Ding, Y., Li, L., Ma, G., Zhang, L., and Jian, B. (2019). A novel molecularly imprinted electrochemical sensor based on double sensitization by MOF/CNTs and Prussian blue for detection of 17 β-estradiol. *Bioelectrochemistry*, 129: 211-217.
- Supchocksoonthorn, P., Alvior Sinoy, M. C., de Luna, M. D. G., and Paoprasert, P. (2021). Facile fabrication of 17β-estradiol electrochemical sensor using polyaniline/carbon dot-coated glassy carbon electrode with synergistically enhanced electrochemical stability. *Talanta*, 235: 122782.
- 41. Salamon, M. N., Mustafa, M. K., and Raja, S. M. N. (2023). The effect of gold and carbon screenprinted electrode (SPE) for biosensing application by electrochemical method. Enhanced Knowledge Sciences in and Technology, 3(2): 255-262.
- 42. Glosz, K., Stolarczyk, A., and Jarosz, T. (2021). Electropolymerised polypyrroles as active layers for molecularly imprinted sensors: Fabrication and applications. *Materials*, 14(6): 1369.
- 43. Shafaat, A., and Faridbod, F. (2022). Overoxidized polypyrrole/ gold nanoparticles composite modified screen-printed voltammetric sensor for quantitative analysis of methadone in biological fluids. *Analytical and Bioanalytical Electrochemistry*, 14(3): 319-330.
- 44. Sravanthi, M., and Manjunatha, K. G. (2020). Synthesis and characterization of conducting polypyrrole with various dopants. *Materials Today: Proceedings*, 46: 5964-5968.
- 45. Pineda, E. G., Azpeitia, L. A., Presa, M. J. R., Bolzán, A. E., and Gervasi, C. A. (2023). Benchmarking electrodes modified with bi-doped polypyrrole for sensing applications. *Electrochimica Acta*, 444: 142011.
- Terán-Alcocer, Á., Bravo-Plascencia, F., Cevallos-Morillo, C., and Palma-Cando, A. (2021). Electrochemical sensors based on conducting polymers for the aqueous detection of

- biologically relevant molecules. *Nanomaterials*, 11: 1-62.
- 47. Dechtrirat, D., Sookcharoenpinyo, B., Prajongtat, P., Sriprachuabwong, C., Sanguankiat, A., Tuantranont, A., and Hannongbua, S. (2018). An electrochemical MIP sensor for selective detection of salbutamol based on a graphene/PEDOT:PSS modified screen printed carbon electrode. RSC Advances, 8(1): 206-212.
- 48. Valentino, M., Imbriano, A., Tricase, A., Della Pelle, F., Compagnone, D., Macchia, E., Torsi, L., Bollella, P., and Ditaranto, N. (2023). Electropolymerized molecularly imprinted polypyrrole film for dimethoate sensing: investigation on template removal after the imprinting process. *Analytical Methods*, 15(10): 1250-1253.
- Ratautaite, V., Boguzaite, R., Brazys, E., Ramanaviciene, A., Ciplys, E., Juozapaitis, M., Slibinskas, R., Bechelany, M. and Ramanavicius, A. (2022). Molecularly imprinted polypyrrole based sensor for the detection of SARS-CoV-2 spike glycoprotein. *Electrochimica Acta*, 403: 139581.
- 50. Mazzotta, E., Di Giulio, T., and Malitesta, C. (2022). Electrochemical sensing of macromolecules based on molecularly imprinted polymers: challenges, successful strategies, and opportunities. *Analytical and Bioanalytical Chemistry*, 414(18): 5165-5200).
- 51. Lah, N. F. C., Ahmad, A. L., Low, S. C., and Zaulkiflee, N. D. (2021). Isotherm and electrochemical properties of atrazine sensing using PVC/MIP: Effect of porogenic solvent concentration ratio. *Membranes*, 11(9): 657.
- 52. Karimi-Maleh, H., Yola, M. L., Atar, N., Orooji, Y., Karimi, F., Senthil Kumar, P., Rouhi, J., and Baghayeri, M. (2021). A novel detection method for organophosphorus insecticide fenamiphos:

- Molecularly imprinted electrochemical sensor based on core-shell Co₃O₄@MOF-74 nanocomposite. *Journal of Colloid and Interface Science*, 592(2):174-185.
- Bolat, G., Yaman, Y. T., and Abaci, S. (2019). Molecularly imprinted electrochemical impedance sensor for sensitive dibutyl phthalate (DBP) determination. Sensors and Actuators, B: Chemical, 299(3): 127000.
- 54. Regasa, M. B., Soreta, T. R., Femi, O. E., Ramamurthy, P. C., and Subbiahraj, S. (2020). Novel multifunctional molecular recognition elements based on molecularly imprinted poly (aniline-co-itaconic acid) composite thin film for melamine electrochemical detection. Sensing and Bio-Sensing Research, 27(12): 100318.
- 55. Pirzada, M., and Altintas, Z. (2021). Template Removal in Molecular Imprinting: Principles, Strategies, and Challenges. *Molecular Imprinting for Nanosensors and Other Sensing Applications*. Elsevier Inc.
- 56. Wu, Y., Li, G., Tian, Y., Feng, J., Xiao, J., Liu, J., Liu, X., and He, Q. (2021). Electropolymerization of molecularly imprinted polypyrrole film on multiwalled carbon nanotube surface for highly selective and stable determination of carcinogenic amaranth. *Journal of Electroanalytical Chemistry*, 895: 115494.
- 57. Marques, G. L., Rocha, L. R., Prete, M. C., Gorla, F. A., Moscardi dos Santos, D., Segatelli, M. G., and Teixeira Tarley, C. R. (2021). Development of electrochemical platform based on molecularly imprinted poly(methacrylic acid) grafted on iniferter-modified carbon nanotubes for 17β-estradiol determination in water samples. *Electroanalysis*, 33(3): 568-578.